DISPLACEMENT OF OIL BY SURFACTANT FLOODING IN MIXED-WET CONDITION

Kumuduni Prasangika Abeysinghe, Ingebret Fjelde and Arild Lohne
International Research Institute Stavanger, Norway

This paper was prepared for presentation at the International Symposium of the Society of core Analysts held in Aberdeen, Scotland, UK, 27-30 August, 2012.

ABSTRACT

Mobilization of capillary trapped oil by lowering the interfacial tension between oil and water by surfactant has shown a great potential in increasing oil recovery at water-wet conditions. Limited knowledge about recovery mechanisms is available for surfactant flooding at mixed-wet conditions.

The main objective of the reported study was to analyze and understand the oil recovery mechanisms in surfactant flooding at mixed-wet condition. For this purpose, unsteady state core floods (water floods and surfactant floods) were carried out in mixed-wet outcrop sandstone rock and reservoir rock materials. Water-oil relative permeability functions were determined by history matching the experimental data, including correction of measured results for capillary end effects. Steady state relative permeability experiments with both oil-water and oil-surfactant solution systems were also carried out at mixed-wet conditions.

Significant tail oil production was observed in unsteady-state water floods in mixed-wet Berea cores. Low residual oil saturation was also confirmed by steady state relative permeability experiment. Reduction in interfacial tension by surfactant increased the estimated oil relative permeability.

Unsteady state water flood in reservoir rock gave tail production similar to the mixed-wet Berea cores. The measured capillary desaturation curve (remaining oil saturation vs capillary number (N_c)) for the reservoir rock showed slowly decline in oil saturation with increasing N_c, with no plateau at low N_c and no critical N_c (N_{cc}).

The importance of capillary end effects in floods carried out to estimate the potential for surfactant flooding should be evaluated. The results indicate no reduction in residual oil saturation with surfactant. The additional oil production was interpreted as a result of increase in k_{ro} at high N_c.

INTRODUCTION

Most of the investigators who have reported on enhanced oil recovery by surfactant have assumed water-wet oil reservoirs. Residual oil left after water flooding is the target for surfactant flooding at water-wet conditions. In water-wet formations, residual oil is trapped as discontinuous droplets due to the capillary forces which prevent oil flow within the pores of rock. The ratio of viscous to capillary forces can be expressed by the dimensionless number, called the capillary number (N_c):

$$N_c = \frac{v\mu}{\sigma} = \frac{viscous\ forces}{capillary\ forces},$$

where ν is the Darcy velocity, μ the viscosity of the displacing fluid and σ is the oil-water interfacial tension. The relationship of residual oil saturation (S_{or}) on N_c can be generalized by the capillary desaturation curve (CDC). In water-wet formations, significant reduction of S_{or} can be achieved by an increase in N_c above critical N_c (N_{cc}). Surfactants are able of reducing σ between oil-water and thereby increase the N_c.

Classic surfactant flooding investigations have been reported utilizing mainly the oil recovery mechanism by reducing the oil-water σ and also assuming the water-wet formations [1, 2]. The wettability of most sandstone reservoirs are characterized as mixed-wet [3-5]. The oil recovery mechanisms using surfactants at mixed-wet conditions have not been investigated to a significant extend. At mixed-wet conditions, remaining oil saturation (ROS) after water flooding is lower than at water-wet conditions.

The objective of this study is to investigate the oil recovery mechanisms by surfactants at mixed-wet conditions. The paper also addresses the importance of correcting experimental results for capillary end effects when evaluating the potential for tertiary oil recovery. This is done by carrying out water floods and surfactant floods in mixed-wet Berea cores and reservoir core using either stock tank oil or n-decane as oil. Unsteady state experiments and one steady-state experiment are performed. History matching and simulations are used in the analyses of the experimental results.

EXPERIMETAL METHOD

Porous Media

Berea sandstone rock and reservoir rock material were used in core flooding experiments.

Chemicals and Fluids

The brine was synthetic formation water (FW) with composition as listed in Table 2. The oils used in were n-decane and stock tank oil (STO). Surfactant solution with σ=0.01 mN/m was prepared with diluted FW (20% FW) due to precipitation problems at higher salinity. 3 vol% Quilon L dissolved in n-decane was used to establish mixed-wet condition in Berea sandstones.

Preparation of Mixed-wet Berea Core Plugs

The core plugs were saturated with FW or 20% FW. Initial water saturation (S_{wi}) was established by draining with N_2 gas using the unconfined porous disc method by gradually increasing the drainage pressure. Then n-decane was injected to replace the N_2 gas. Quilon L in n-decane was injected at 0.5 ml/min in both directions. Afterwards, n-decane was injected to remove the excess treatment chemicals.

Preparation of Reservoir Core Plug

The core plug was cleaned by injecting toluene and methanol at 60°C until the effluent solution was colourless. Cleaning cycles of toluene followed by methanol were used. The methanol in the plug was replaced with FW. The cleaned 100% water saturation plug was drained to S_{wi} with Isopar H (white oil) at room temperature using the confined porous

disc method. A constant over-burden pressure of 50 bar was kept during the drainage process. Wettability was established by continuously injecting stock tank oil (STO). This was done by first injecting a mixture of Isopar H/toluene and next STO (5PV) at 90^{o}C. A constant injection rate of 0.5 ml/min was used. The plugs were aged at 90^{o}C for 14 days. The reason for aging at higher temperature (90^{o}C) than the reservoir temperature (38 ^{o}C) was to accelerate the reaction between crude oil components and the rock material.

Core Flooding Procedure for Berea Core Plugs

Unsteady State Experiments: Core floods were carried out at 38°C horizontally with an overburden pressure of 50 bar and a back pressure of 10 bar.

Water floods: FW was injected to the mixed-wet core plugs at S_{wi}. Single flow rate or multiple flow rates were used as listed in Table 1.

Surfactant floods: Surfactant solution was injected to the core plugs at S_{wi} at 3.0 ml/min.

Steady State Experiments: Experiment was carried out at 38°C with an overburden pressure of 50 bar and a back pressure of 20 bar. The core was mounted vertically, and the fluids were injected upwards. The water fraction was increased in 8 steps from zero to one. Differential pressure and oil production were measured during the experiment, and relative permeability was calculated with Darcy law at each steady state condition.

Core Flooding Procedure for Reservoir Core Plug

Core floods were carried out at 38°C horizontally with an overburden pressure of 50 bar and a back pressure of 10 bar. A single core sample was used for both water flooding and surfactant flooding experiments. FW was injected to the core plug at S_{wi} with gradually increasing the injection rate from 0.3, 1.0, 3.0 to 7.0 ml/min. After the water flood, surfactant solution was injected at multiple rates (0.1, 0.3, 1.0, 3.0 and 7.0 ml/min).

SIMULATION METHOD

The simulations were carried out using the Sendra simulator. Sendra utilizes a fully implicit black oil formulation based on Darcy's law and continuity equation [6]. It can be run with an automated history matching routine (estimation mode) or as a standard simulator producing a forward simulation of an experimental performance (simulation mode). Both modules were employed in this study. The simulation was carried out on a block centered grid, describing oil displacement by water flood in 1 dimension.

Relative permeability (k_r) functions and capillary pressure curves were estimated by history matching the oil recovery and the pressure drop data obtained from the core floods. The LET correlation [7] was used to represent the water-oil k_r curves. The capillary pressure curves were represented using Skjæveland's model [8]. Absolute permeability measured with brine was used as the base permeability to estimate the relative permeability to a phase.

The relative permeability in the steady-state experiment was corrected for capillary end effects using the steady state simulator Coreflow [9].

RESULTS AND DISCUSSION

Table 1 provides the properties of the core plugs used in the core flooding experiments. Properties of the fluid are listed in Table 3. The core flooding experiments discussed in this paper are mainly unsteady state water and surfactant displacement studies carried out on mixed-wet core samples. The remaining oil saturation after water flooding is denoted ROS to distinguish it from the final microscopic S_{or}. The ROS represents a practical cut-off value of the average oil saturation when fractional production of oil approaches zero, and it can be significantly higher than S_{or} in mixed-wet cores.

In this study, the wettability treatment was done at S_{wi} (after drainage) in order to obtain mixed-wet Berea cores (smaller pores remains water-wet and larger pores changing to oil-wet). Established wettability conditions on Berea samples were characterized by several tests including resistivity saturation exponent (n), spontaneous imbibition of brine and Nuclear Magnetic Resonance (NMR) Relaxation test. Details about characterization of wettability for similar core samples can been found in a previous publication [13]. The wettability conditions on treated Berea core plugs have also been cross checked by NMR Relaxation and the shift in T2 was observed compared to untreated core plugs (unpublished data).

Unsteady state core floods on Berea sandstone rock samples

Figure 1 shows ROS plotted versus PV injected for the three core floods using n-decane as oil. The multi-rate case (Berea 2) clearly shows a rate dependent production, where ROS approaches a constant level at each rate. When the rate is increased, there is an immediate increase in the oil fractional flow, and stabilization of ROS at a lower value. One may also observe that the ROS in the single-rate water injection case (Berea 1) coincide with the corresponding ROS level in the multi-rate case (1 ml/min). In the surfactant case (Berea 3), a higher and faster oil production is observed.

Plotting of oil production (or ROS) versus volume injected is a convenient way of revealing rate dependency of the core system. If the production is rate independent, the production profile would be smooth without any jumps when the rate is changed. The observed rate dependency in Figure 1 can be explained by that the relative permeabilities themselves are rate dependent or that the production is affected by capillary forces. Rate dependency in the relative permeability functions is normally expected at high N_c values above approximately 10^{-5} [9, 14]. In this case (Berea 2), N_c ranged from $3.2 \cdot 10^{-8}$ to $3.2 \cdot 10^{-6}$, and the rate dependency is assumed to be caused by capillary end effects.

The influence of capillary forces is demonstrated by the simulated saturation profiles in Figure 2. In the high σ case (Berea 1, $N_c=3.2 \cdot 10^{-7}$), a significant saturation gradient along the core length can be seen while after suppressing the capillary forces with surfactant (Berea 3, σ =0.01 mN/m, $N_c=3.8 \cdot 10^{-3}$) no /less saturation gradient exhibits. Rate dependent ROS values observed in water flooding of Berea 2 (Figure 1) is most likely due to the elimination of capillary end effects with the increase of flow rate. Capillary end effects in the core floods are purely laboratory artifacts. It is vital that experimental

core flooding data at mixed-wet or non-water-wet conditions must be corrected for capillary end effects.

Oil-water k_r curves and P_c curve were estimated by history matching the experimental data from the water flood of Berea 2. Simulated flow functions are plotted in Figure 3 together with the history matched ROS and differential pressure (DP) data. P_c curve is positive for low S_w and negative for high S_w. Both k_{rw} and k_{ro} show high curvature. Note that the main output from the history matching is the relative permeability functions. The primary purpose of estimating the capillary pressure is to correct the computed relative permeability for the influence of the capillary pressure. As seen in Figure 3a, the rate dependent behavior is quite well reproduced using the computed rate-independent relative permeability functions and estimated P_c given in Figure 3b.

Ideally, the capillary pressure should be measured independently. In the present case (Berea 2 in Figure 3), the estimated S_w (P_c=0) is higher than the value measured by spontaneous imbibition as reported in our previous work [13]. It also seems that Sendra tends to estimate an S_{or} very close to the experimental ROS (0.018 saturation units below in this case), so that the influence of capillary end effects is overestimated for the last rate. This is best seen on the DP-profile in Figure 3a, where the declining slope towards the end is not matched. It is assumed that the steep declining P_c should occur at a substantially higher S_w, which is supported by the steady-state results (Berea 7) presented in a later section.

The capillary correction of computed relative permeability can be split into two parts. First, there may be an additional pressure drop towards the outlet end of the core if k_{rw} is very low at the outlet saturation S_w (P_c=0). This results mainly in a correction (increase) of the k_r level for both oil and water. Then, after sufficient injection, the capillary pressure will increase at the inlet and approach DP, at which point the internal oil pressure gradient becomes zero and the oil production is terminated. The second correction has its major influence on the computed k_{rw}/k_{ro} ratio, which is important for the predicted production profile when scaling to larger dimensions. Because of the uncertainty in the estimated P_c, computed k_r must be regarded as a non-unique solution, however, the reproduction by simulation of the rate dependency in the oil production profile (ROS) indicates a reasonable correction for the second mechanism, (the influence of capillary end effects on the production profile) with some overcorrection towards the end (highest rate).

Another set of core floods (both water flood and surfactant flood from S_{wi}) were carried out in similar mixed-wet Berea core plugs with STO as oil. Figure 4a shows ROS as a function of PV's injected for these floods. In the water flood experiments (Berea 4 and 5), much higher ROS values were observed compared to when n-decane was displaced (see Figure 1). The reason for this difference is the higher viscosity ratio of oil to water when STO is used. To displace high viscous oil, much higher throughput of water is required. In the multiple rate water flood experiment (Berea 5), no significant production jumps

can be seen in the ROS profile. This may be explained by reduced influence of capillary forces at lower average S_w compared to when low viscous n-decane is displaced (Figure 3a). This is also a strong indication of that the tail oil production, which is not completed at the end of the experiment, is essentially limited by the relative permeability rather than by capillary end effects.

The lack of capillary influence on the oil production profile makes it impossible to obtain reliable estimations of P_c. Instead, P_c curve estimated from the water flood of Berea 2 is used in history matching the experimental data of Berea 4, Berea 5 and Berea 6 (after scaling for differences in σ). The matched DP and ROS history is shown in Fiure 4b and 4c. Estimated k_r functions are plotted in Figure 4 (d). Assuming that the applied P_c gives a reasonable correction to the k_{rw}/k_{ro} ratio (and hence the oil production profile), only a small part of the increased oil production with surfactant can be explained by removal of capillary end effects at low σ alone. The main part of the increased oil production requires also an improved (reduced) k_{rw}/k_{ro} ratio, seen mainly as an increased k_{ro}.

No reduction in S_{or} can be deduced from the results, contrary, the combined experimental results from all the similar cores indicates that ROS in the surfactant flooding is still far above S_{or} that can be obtained by water flooding. This indicates that the main surfactant mechanism at mixed-wet conditions is accelerated oil production due to increased k_{ro} at high N_c and not necessarily involving a reduction in S_{or}.

The pressure was increasing at the end of surfactant flood of sample Berea 6. This could be due to the formation of macroemulsion inside the core especially at high injection rate.

Estimated k_r curves may also suffer from limitations in the capability of the selected correlation to represent the true k_r curves. Also there is less experimental support for the section before the breakthrough. However we are primarily interested in the shift in k_r curves by the surfactant, which indicates the acceleration of the oil production.

Figure 5 shows water flood estimated k_r curves for Berea 2 (n-decane as oil) and Berea 5 (STO as oil). The results appear to be quite different for similar core samples but with different oil types. However, the ratio of k_{rw}/k_{ro} is similar for the two core floods (Berea 2 and Berea 5) indicating that the two set of curves will result in approximately the same oil production, however DP would be different. The k_{rw}/k_{ro} ratio from the surfactant flood (Berea 6) has a lower slope and indicates faster (accelerated) oil production.

Steady state core floods on Berea sandstone rock samples

Oil-water k_r curves were measured using steady state technique to derive the k_r curves in the broad saturation range. Unsteady state method is the classic method to measure k_r curves, with the advantages of being rapid and simple. However this method has very strong limitations such as narrow saturation range and capillary end effects. The steady state method is a complex and time consuming technique compared to the unsteady state method. But it gives k_r information in a broader saturation range. The measured steady state k_r curves are shown in Figure 6. It covers saturation range from 0.1 to over 0.8. A good history matching was obtained by Coreflow. The experimental pressure drop indicated a slow reduction in the core permeability versus volume injected during the

injection of two phases (not shown). This was not experienced in unsteady state experiments. Measured k_r curves show mixed-wet behavior and corroborate the possibility of measuring k_r in a larger saturation range. It is also interesting to see that k_{ro} becomes very low towards the S_{or}. The steady state experiment demonstrates that the cutoff values estimated by Sendra are not very accurate and S_{or} should be lower. In the measurement of steady state oil-surfactant k_r curves, plugging problems occurred. This was probably due to the formation of macro emulsions inside the core. More work is needed to further understand this behavior and propose necessary modifications to the injection procedure.

Unsteady state core floods on a reservoir rock sample

The reservoir core plug was selected on the basis of having relatively homogeneous computerized tomography (CT) –scan images. Both ROS and DP profiles during water flooding of the reservoir core are shown in Figure 7 (a) together with the history matched profiles. Estimated k_r curves by Sendra using P_c curve measured on other reservoir sample (from same reservoir) are plotted in Figure 7 (b). Estimated flow functions show a typical mixed-wet behavior. Surfactant flooding was carried out after the water flooding with stepwise increase in the flow rate, as listed in Table 1. In order to minimize the uncertainty in saturation caused by oil solubilization, surfactant solution after equilibrium with STO was used in the surfactant flooding experiment. Measured ROS vs N_c is shown in Figure 8. Declining slope at low N_c (water flooding) is mainly due to the capillary end effects and the number of PV injected in the experiment. A gentle slope was observed at high N_c (surfactant flooding). At mixed-wet or weakly water-wet conditions, S_{or} is difficult to obtain in core flooding experiments [4, 10]. Remaining oil left after water flooding is still mobile since ROS after water flooding, is higher than S_{or}. Assuming the capillary pressure curve used in the history matching of the relative permeability is correct, ultimate recovery in surfactant flood is given by the steady state solution [11] plotted in Figure 8. The shape of the limiting steady-state curve will also depend on the core length and it is assumed that oil mobility is positive between the asymptotic limits of the P_c curve. At saturations close to the limiting curve, capillary end effects are important. Further above the curve, the oil production is mainly limited by low k_{ro} and ROS depends on number of PV injected. During surfactant flooding, reduction of ROS can be partly due to the number of PVs injected. Based on the experience with mixed-wet Berea core plugs, the reduction in ROS can also be due acceleration of oil production by improvement of relative permeability. Similar non representative CDC shapes were also observed in our previous studies [12, 13]. Therefore plotting the measured ROS values vs N_c does not represent the true CDC behavior. In mixed-wet or non water-wet conditions, the most important effect of surfactants can be the acceleration of oil; not necessarily the reduction of S_{or}.

CONCLUSIONS

Water flooding experiments with mixed-wet Berea cores gave tail production due to low k_{ro} and the results were highly influenced by capillary end effects. Low residual oil saturation was confirmed by steady state relative permeability experiment.

Surfactant flooding experiments in mixed-wet Berea cores showed additional oil production compared to the water flooding experiments, but results show no indication of reduction in residual oil by the surfactant. The results were interpreted as acceleration of oil production due to increase in oil relative permeability when the capillary number was increased.

Water flooding of reservoir rock also showed tail production similar to the mixed-wet Berea. The measured remaining oil saturation declined slowly with capillary number indicating no So-plateau at low N_c and no N_{cc}.

In evaluation of the potential for surfactant flooding, the importance of capillary end effects in flooding experiments should be evaluated. Based on the results in mixed-wet Berea and reservoir core no conclusion can be drawn about the effect of surfactant on the residual oil saturation. The additional oil production was interpreted as a result of increase in k_{ro} at high N_c.

ACKNOWLEDGEMENTS

The authors want to thank Wintershall Holding GmbH and Norwegian Research Council for supporting this work.

REFERENCES

1. Iglauer, S., Y. Wu, P. Shuler, Y. Tang and W. A. Goddard III, "New Surfactant Classes for Enhanced Oil Recovery and Their Tertiary Oil Recovery Potential," *Journal of Petroleum Science and Engineering,* (2010) **71**, 23-29.
2. Stoll, W. H., H. al Shureqi and J. Finol, "Alkaline/Surfactant/Polymer Flood: From the Laboratory to the Field", *SPEREE*, (2011), 702-712.
3. Salathiel, R. A., "Oil Recovery by Surface Film Drainage in Mixed-Wettability Rocks," *Journal of Petroleum Technology*, (1973) **255**, 1216-1224.
4. Wood, A.R. and T. C. Wilcox, "Determining Effective Residual Oil Saturation for Mixed Wettability Reservoirs: Endicott Field, Alaska," SPE 22903, SPE Annual Technical Conference and Exhibition, 6-9 October 1991, Dallas, TX.
5. Agbalaka, C., A. Y. Dandekar, S. L. Patil, S. Khataniar and J. R. Hemsath, "The Effect of Wettability on Oil Recovery: A Review," SPE 114496, SPE Asia Pacific Oil & Gas Conference and Exhibition, 20-22 October 2008, Perth, Australia.
6. Sendra simulator user guide version 2011.3, www.sendra.no.

7. Lomeland, F., E. Ebeltoft and W. H. Thomas, "A New Versatile Relative Permeabiliy Correlation," the International Symposium of the Society of Core Analysts held in Toronto, Canada, 21-25 August 2005.
8. Skjaeveland, S.M., L. M. Siqveland, A. Kjosavik, W. L. Hammervold Thomas and G. A. Virnovsky, "Capillary Pressure Correlation for Mixed-Wet Reservoirs," SPE Reservoir Evaluation & Engineering, (2000) **3**, 60–67.
9. Virnovsky, G.A., Vatne, K.O., Skjæveland, S.M., and Lohne, A. "Implementation of Multirate Technique to Measure Relative Permeabilities Accounting for Capillary Effects", SPE 49321, SPE Annual Technical Conference and Exhibition, New Orleans, Louisiana, 27-30 September, 1998.
10. Sorbie, K. S., A. V. Ryazanov and M. I. J. Dijke, "The Structure of Residual Oil as a Function of Wettability Using Pore-Scale Network Modelling," Paper SCA2011-37, the International Symp. of the Society of Core Analysis held in Austin, Texas, USA, 18 – 21 September 2011.
11. Kyte, J. R. and L. A. Rapport, "Linear Water Flood Behaviour and End Effects in Water-Wet Porous Media," Petroleum Transactions AMIE, (1958) **213**, 423-426.
12. Chukwudeme, E. A., I. Fjelde, K. Abeysinghe and A. Lohne, "Effect of Interfacial Tension on Water/Oil Relative Permeability and Remaining Saturation with Consideration of Capillary Pressure," SPE 143028, the SPE EUROPEC/EAGE Annual Conference and Exhibition, 23-26 May 2011, Vienna, Austria.
13. Abesinghe, K. P., I. Fjelde and A. Lohne, "Dependency of Remaining Oil Saturation on Wettability and Capillary Number," SPE 160883, SPE Saudi Arabia Section Techn. Symp. & Exhib., 8-11 April 2012, Alkhobar, Saudi Arabia.
14. Lake, L. W. (1989). Enhanced Oil Recovery, Prentice-Hall, Inc.

Table 1. Core properties

Core No.	L (cm)	D (cm)	PV (ml)	Φ (fraction)	k_{abs} (mD)	S_{wi}	k_{ro}	Q (ml/min)	Core flood	Oil
Berea 1	8.93	3.77	22.27	0.22	533	0.08	0.44	1.0	WF	n-decane
Berea 2	8.98	3.77	23.60	0.24	418	0.10	0.64	0.1→0.3→1→3→10	WF	n-decane
Berea 3	9.01	3.77	22.48	0.22	657	0.06	0.37	3.0	SF	n-decane
Berea 4	8.96	3.79	22.04	0.22	537	0.07	-	1.0	WF	STO
Berea 5	9.03	3.77	22.56	0.22	562	0.09	0.45	1.0→3.0→7.5	WF	STO
Berea 6	8.98	3.79	22.50	0.22	608	0.06	0.43	3.0	SF	STO
Berea 7	8.91	3.75	22.39	0.23	588	0.08	1.08	Steady state 2.0 ml/min	WF	n-decane
Reservoir core	9.15	3.01	16.33	0.25	508	0.29	-	0.3→1→3→7	WF	STO
								0.1→0.3→1→3→7	SF*	STO

* Surfactant injected after the water flood

Table 2. Brine composition

Salt	Units	FW
$CaCl_2 \cdot 2H_2O$	g/L	37.6
$MgCl_2 \cdot 6H_2O$	g/L	15.0
NaCl	g/L	88.0
Na_2SO_4	g/L	0.2

Table 3. Properties of Fluids at 38 ºC

Fluid	Density (g/cm³)	Viscosity (cP)	σ with STO (mN/m)	σ with n-decane (mN/m)
FW	1.08	0.86	22	40
n-d cane	0.73	0.72	-	-
STO	0.88	35	-	-
0.4 wt% surfactant solution	1.01	0. 5	0.01	0.01

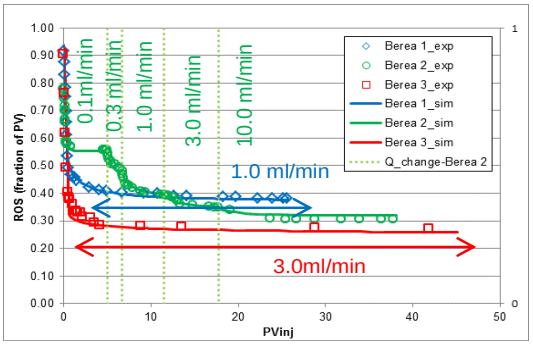

Figure 1. Remaining oil saturation during water flooding (Berea 1_single rate & Berea 2_multiple rate) and surfactant flooding (Berea 3_single rate): n-decane as oil.

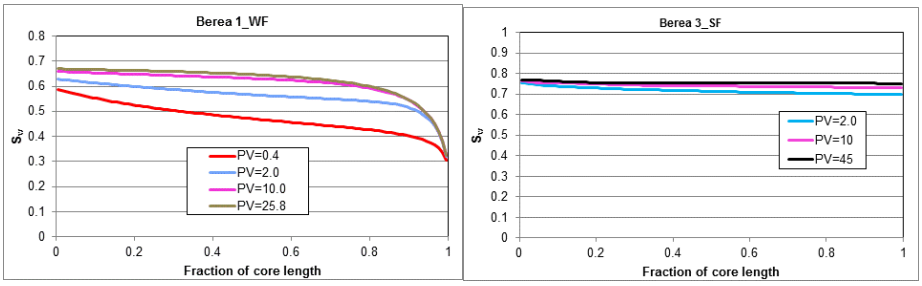

Figure 2. Simulated insitu S_w distribution during water flooding and surfactant flooding.

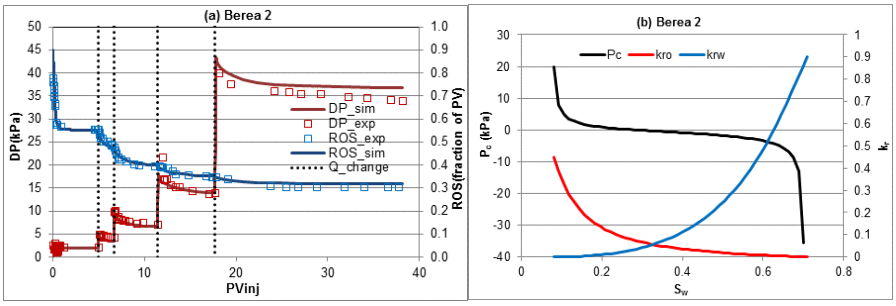

Figure 3. (a) ROS and ΔP profiles and (b) estimated k_r and P_c curves during WF in mixed-wet Berea (n-decane as oil) [13]

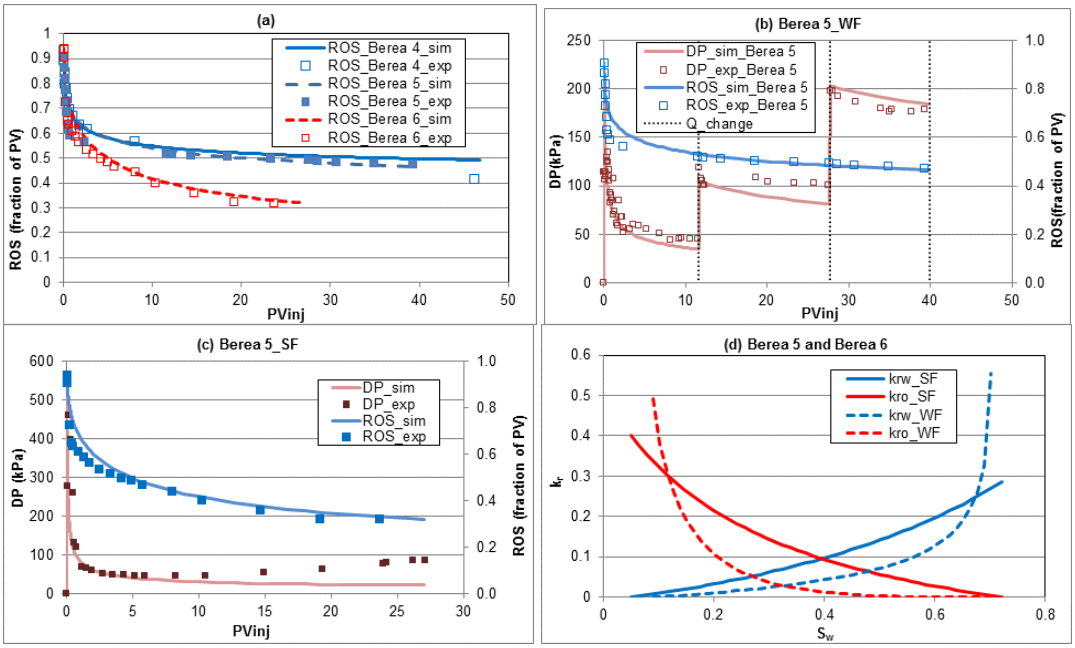

Figure 4. Results from water and surfactant floods in mixed wet cores using STO as oil, experimental and simulated ROS and DP history (a-c) and computed k_r (d).

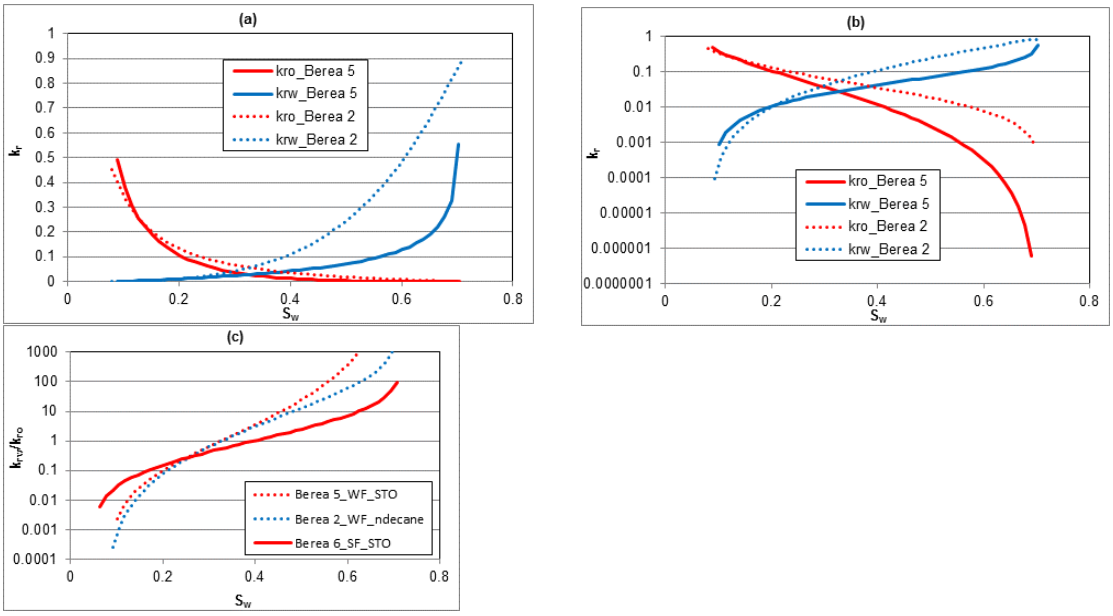

Figure 5. (a) Estimated k_r curves from waterfloods with n-decane (Berea 2) and STO (Berea 5) and (c) corresponding k_{rw}/k_{ro}-ratios compared to surfactant flood in Berea 6.

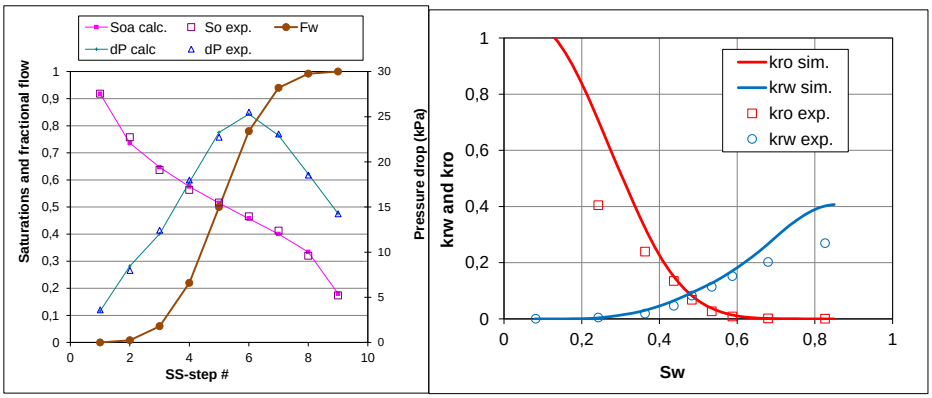

Figure 6 (a) History match of steady state data: pressure drop (DP) and oil production (OP) (b) Steady state oil-water relative permeability curves (Berea 7).

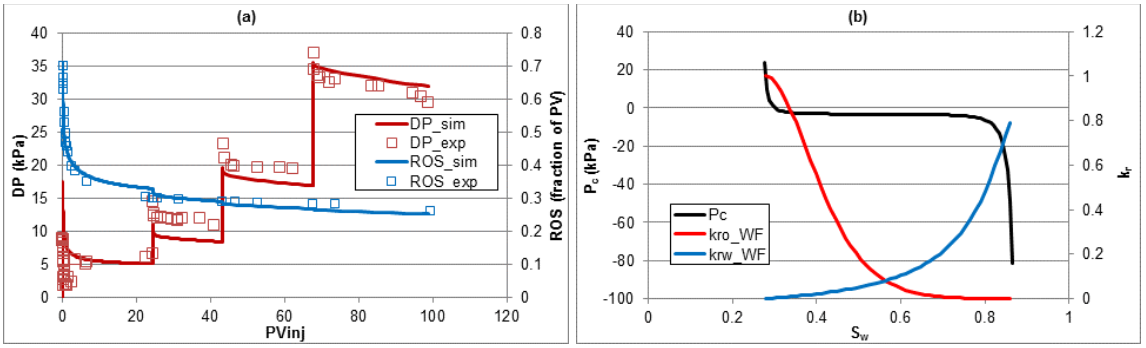

Figure 7. (a) Remaining oil saturation and differential pressure during water flooding of Reservoir core (b) Oil-water relative permeability and capillary pressure curves for the reservoir core.

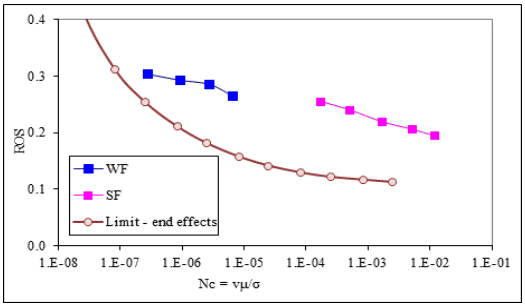

Figure 8 Measured ROS vs N_c during water flooding and surfactant flooding in reservoir core. Steady state (SS) limit indicates the lowest ROS for the core system if there is no reduction in S_{or}.